

Concentration and relaxation depth profiles of $\text{In}_x\text{Ga}_{1-x}\text{As}/\text{GaAs}$ and $\text{GaAs}_{1-x}\text{P}_x/\text{GaAs}$ graded epitaxial films studied by x-ray diffraction

A. Benediktovitch

Department of Theoretical Physics, Belarusian State University, 4 Nezavisimosti av., 220030 Minsk, Belarus

A. Ulyanenko and F. Rinaldi

Bruker AXS GmbH, Östliche Rheinbrückenstr. 49, 76187 Karlsruhe, Germany

K. Saito

Bruker AXS K.K., 3-9 Moriya, Kanagawa, 221-0022 Yokohama, Japan

V. M. Kaganer

Paul-Drude Institut für Festkörperelektronik, Hausvogteiplatz 5-7, 10117 Berlin, Germany

(Received 30 March 2011; revised manuscript received 8 June 2011; published 12 July 2011)

A method is proposed to determine the concentration and relaxation depth profiles in graded epitaxial films from x-ray reciprocal space maps (RSMs). Various approximations in the kinematical x-ray diffraction from epitaxial films with the misfit dislocation density depth profile are developed. We show that a symmetric and an asymmetric RSM, or two asymmetric RSMs, contain enough information to obtain the concentration, relaxation, and lattice tilt depth profiles without any additional assumptions. The proposed approach is applied to $\text{In}_x\text{Ga}_{1-x}\text{As}/\text{GaAs}$ and $\text{GaAs}_{1-x}\text{P}_x/\text{GaAs}$ epitaxial graded films. The reconstructed concentration and dislocation density depth profiles are found to be in an agreement with the ones expected from the growth conditions.

DOI: [10.1103/PhysRevB.84.035302](https://doi.org/10.1103/PhysRevB.84.035302)

PACS number(s): 61.05.cp, 68.35.-p, 61.72.Dd, 61.72.Lk

I. INTRODUCTION

High-resolution x-ray diffraction is a standard tool to measure the relaxation in epitaxial films. For uniform layers, a comparison of the diffraction peak positions on the reciprocal space maps (RSMs) taken in a symmetric and in an asymmetric reflection provides the lattice parameter of the film and the degree of relaxation.¹ The problem becomes more complicated for layers containing the lattice parameter gradients due to concentration variations. Instead of separate peaks from uniform layers on the RSMs, one observes in the graded layers a continuous intensity distribution.

The determination of the concentration and relaxation profiles from graded epitaxial films on the basis of RSM measurements is not straightforward. It has been performed by introducing additional simplifying assumptions.²⁻⁵ Holy *et al.*² suggested to subdivide the RSM into slices parallel to the film surface, and consider the intensity maximum position for a slice as a diffraction peak position due to corresponding layer in the film. This approach has a severe restriction in resolution, which remains evident if one attempts to treat the RSM from a uniform relaxed layer in the same way. The misfit dislocations at the layer interface give rise to broad (with the width increasing as a square root of the dislocation density) spots, approximately described by an anisotropic Gaussian intensity distribution.⁶ Their interpretation in the same way as suggested for the graded layer would result in a continuous (approximately Gaussian) variation of the concentration, instead of the abrupt change in the experiment. Even with this resolution restriction in mind, this method² delivers the relaxed lattice parameter and the misfit dislocation density of the film sublayer corresponding to the given slice of RSM. The depth position of this sublayer cannot be directly determined from the x-ray data and needs a preliminary

knowledge of the concentration profile. Danis *et al.*⁵ avoided the use of a known concentration profile but introduced an assumption on the relation between the concentration and the dislocation density profiles. They suggested that the relaxation corresponds to the minimum of elastic energy, so that the dislocation density is given by the concentration gradient.

The aim of the present work is to determine the concentration and the dislocation density profiles from RSMs of graded epitaxial films without assuming any relations between these profiles and using the RSM intensity distributions only.

II. CALCULATION OF RECIPROCAL SPACE MAPS

The relaxation of graded epitaxial films occurs by creation of misfit dislocations parallel to the interface. The areal dislocation density is the number of dislocation lines per unit area in the plane perpendicular to the dislocation lines. For a (001) oriented cubic crystal, there are two orthogonal sets of parallel dislocation lines, we take the directions of which as x and y axes. For each set of dislocations, the density is

$$\rho(z) = \frac{1}{b_x a_x(z)} \frac{da_x(z)}{dz}, \quad (1)$$

where $a_x(z)$ is the lattice spacing in the plane of interface in the direction perpendicular to the dislocation line, and b_x is the Burgers vector component that provides the relaxation. Here the z axis is along the normal to the plane of the interface. For typical gradient layers, e.g., virtual substrates, the dimensionless parameter ρd^2 , where d is the layer thickness, varies between 10^1 and 10^3 . The static Debye-Waller factor $e^{-\rho d^2}$ is negligibly small and the dynamical x-ray scattering effects can be neglected. Thus, the theory below is restricted with the kinematical approximation.

The relaxation of the graded epitaxial films can also be characterized by the relaxation parameter $R(z)$ defined with respect to the substrate:

$$R(z) = \frac{a_x(z) - a_x^{(s)}}{a_x^{(0)}(z) - a_x^{(s)}}, \quad (2)$$

where $a_x^{(s)}$ is the substrate lateral lattice parameter, $a_x^{(0)}(z)$ is the lateral lattice parameter which the film would have if at depth z it were completely relaxed. The value $a_x^{(0)}(z)$ for a two-component solid solution alloy A_xB_{1-x} can be found from concentration $c(z)$ at depth z , e.g., using Vegard's law: $a_x^{(0)}(z) = c(z)a_A + [1 - c(z)]a_B$. In this case, it follows from Eq. (1) that dislocation density, relaxation, and concentration profiles are connected by

$$R(z) = \frac{b_x \int_0^z \rho(z') dz'}{\epsilon c(z)}, \quad (3)$$

where $\epsilon = (a_A - a_B)/a_B$ is the crystal lattice mismatch between materials A and B. The difference of the lattice parameters a_A and a_B is assumed here to be small, $\epsilon \ll 1$.

The displacement of atoms from their positions in ideal periodic lattice taken as a reference consists of two contributions. One is the displacement with respect to the substrate in a fully pseudomorphic layer. For the two-component solid solution alloy A_xB_{1-x} , the displacement gradient is proportional to the concentration $c(z)$ of the component A and can be written, using Vegard's law and assuming isotropic elasticity, as⁵

$$\frac{du_z^p(z)}{dz} = \frac{1 + \nu}{1 - \nu} \epsilon c(z), \quad (4)$$

where ν is the Poisson ratio. The z -component (4) is the only nonzero component of the displacement \mathbf{u}^p .

The other contribution to the displacement is due to displacement fields of the misfit dislocations. We denote by $\mathbf{u}(x, z; z')$ the displacement field at the point (x, z) due to the dislocation going through the point $(0, z')$. The dislocation line is along y axis. The displacement field can be represented, taking into account the elastic relaxation at the free surface, as⁶

$$\mathbf{u}(x, z; z') = \mathbf{u}^\infty(x, z - z') - \mathbf{u}^\infty(x, z + z') + \mathbf{u}^{\text{surf}}(x, z + z'), \quad (5)$$

where $\mathbf{u}^\infty(x, z)$ is the displacement field in the infinite medium of a dislocation at origin. The first two terms in Eq. (5) correspond to the dislocation itself and image with respect to the surface, and the third term is the remaining surface relaxation. The explicit expressions for all these terms and for all Burgers vector orientations are given in Appendix B of Ref. 6.

The diffracted x-ray intensity distribution from layer with dislocations at interface was considered in Ref. 6. In this work, we extend this approach on the case of graded layers. The next two paragraphs summarize information from Ref. 6 that is needed further.

Taking into account the two contributions to the displacement field, Eqs. (4) and (5), and the dislocation distribution

over the film, the general expression for the scattered x-ray intensity can be represented as

$$I(q_x, q_z) = \int_0^d \int_0^d dz_1 dz_2 \int_{-\infty}^{\infty} dx e^{iq_x x + iq_z(z_2 - z_1)} \times e^{i\mathbf{Q} \cdot (\mathbf{u}^p(z_2) - \mathbf{u}^p(z_1))} G(x, z_1, z_2), \quad (6)$$

where d is the film thickness, \mathbf{Q} is the scattering vector, $\mathbf{q} = \mathbf{Q} - \mathbf{Q}^{(s)}$ is deviation of the scattering wave vector from reciprocal-lattice point $\mathbf{Q}^{(s)}$ of the substrate, and $G(x, z_1, z_2)$ is the correlation function due to dislocation displacements. It originates from displacements caused by randomly distributed dislocations. Assuming that the dislocation positions are not correlated, one can represent the correlation function for dislocations of one type (the dislocations that have the same direction and the same Burgers vector) as (see also Refs. 7 and 8)

$$G(x, z_1, z_2) = \exp[T(x, z_1, z_2)], \quad (7)$$

where

$$T(x, z_1, z_2) = \int_0^d dz' \rho(z') \tau(x, z_1, z_2, z') \quad (8)$$

and

$$\tau(x, z_1, z_2, z') = \int_{-\infty}^{\infty} dx' (e^{i\mathbf{Q} \cdot [\mathbf{u}(x' + x, z_2; z') - \mathbf{u}(x', z_1; z')]} - 1). \quad (9)$$

Numerical calculations that directly use the general expressions (7)–(9) occur very cumbersome. For relaxed uniform layers, with misfit dislocations located at the interface,⁶ the main contribution to the integral (9) is due to closely located points, so that the difference of displacements can be expanded:

$$\begin{aligned} & \mathbf{u}(x' + x, z_2; z') - \mathbf{u}(x', z_1; z') \\ & \approx \frac{\partial \mathbf{u}(x', z_1; z')}{\partial x'} x + \frac{\partial \mathbf{u}(x', z_1; z')}{\partial z_1} \zeta, \end{aligned} \quad (10)$$

where we denote $\zeta = z_2 - z_1$. As a result, the imaginary part of the function $\tau(x, z_1, z_2, z')$ is linear over x and ζ ,

$$\begin{aligned} & \text{Im } \tau(x, z_1, z_2, z') \\ & = \int_{-\infty}^{\infty} dx' \mathbf{Q} \cdot \left[\frac{\partial \mathbf{u}(x', z_1; z')}{\partial x'} x + \frac{\partial \mathbf{u}(x', z_1; z')}{\partial z_1} \zeta \right], \end{aligned} \quad (11)$$

and leads to shift of the peak center according to average strain of the layer lattice, while the real part is quadratic over these distances:

$$\text{Re } \tau^{(2)}(x, z_1, z_2, z') = -[w_{11}x^2 + 2w_{12}x\zeta + w_{22}\zeta^2]. \quad (12)$$

Here it is denoted

$$w_{11}(z, z') = \frac{1}{2} \int_{-\infty}^{\infty} dx' \left(\mathbf{Q} \cdot \frac{\partial \mathbf{u}(x', z; z')}{\partial x'} \right)^2, \quad (13)$$

the functions $w_{12}(z, z')$ and $w_{22}(z, z')$ are defined similarly⁶ by making derivatives over z instead of the derivatives over x' . The quadratic form of the real part of T in the case of uniform relaxed layers leads to anisotropic Gaussian shape of diffracted peak with the minor axis parallel to the diffraction vector \mathbf{Q} . The real part $\text{Re } \tau$ is denoted in Eq. (12) as $\text{Re } \tau^{(2)}$ to indicate the expansion quadratic over x and ζ .

The expansions (11) and (12) are accurate enough to calculate the x-ray diffraction peaks from uniform relaxed films with misfit dislocations located at the interface. However, for dislocations distributed in the film, we find that the coefficients $w_{ij}(z, z')$ (here $i, j = 1, 2$) diverge at $z' \rightarrow z$ as $w_{ij}(z, z') \propto |z - z'|^{-1}$. As a result, this approximation leads to an erroneous divergence of the integral (8), while in an accurate calculation, the integral converges. The same problem arose for uniformly distributed dislocations in Ref. 11. In this latter case, the contribution to the correlation function from small separations was estimated and used to renormalize the contribution from the upper limit of the integral. Since this upper limit was an ill-defined crystallite size, its change was not important. In the present case, however, the contribution from the lower limit is essential and the upper limit is a well-defined film thickness.

The singularity of the function $w_{ij}(z, z')$ at $z' \rightarrow z$ appears since the expansion (10) becomes invalid. In the limit $z' \rightarrow z$, numerical calculations show that the real part $\text{Re } \tau(x, z_1, z_2, z')$ is well approximated by the expression

$$\begin{aligned} \text{Re } \tau^{(1)}(x, z_1, z_2, z') \\ \approx -\sqrt{x^2 + \zeta^2} [a_0 + a_1 \cos(2\phi) + a_2 \sin(2\phi)], \end{aligned} \quad (14)$$

where $\phi = \arctan(\zeta/x)$ and the coefficients $a_i(z, z')$ ($i = 1, 2, 3$) remain finite at $z' \rightarrow z$ and decrease as the distance $|z - z'|$ increases. $\text{Re } \tau$ is denoted as $\text{Re } \tau^{(1)}$ in this approximation, to indicate that it is linear over x and ζ .

We have numerically calculated the function of four arguments $\tau(x, z_1, z_2, z')$ and fitted its real part to the sum $\text{Re}(\tau^{(1)} + \tau^{(2)})$ given by Eqs. (14) and (12). The result of the fit is three functions $w_{ij}(z, z')$ ($i, j = 1, 2$) and three functions $a_i(z, z')$ ($i = 1, 2, 3$). We find that w_{ij} decrease to zero at $z' \rightarrow z$, while a_i are maximal in this limit and decrease when the distance $|z - z'|$ increases.

The imaginary part $\text{Im } \tau(x, z_1, z_2, z')$ is well approximated by Eq. (11), and the integrals can be calculated analytically.⁶

$$\text{Im } \tau(x, z_1, z_2, z') \approx -i[\delta\tilde{q}_x(z, z')x + \delta\tilde{q}_z(z, z')\zeta], \quad (15)$$

where

$$\begin{aligned} \delta\tilde{q}_x(z, z') &= Q_x b_x H(z - z'), \\ \delta\tilde{q}_z(z, z') &= -\frac{2\nu}{1-\nu} Q_z b_x H(z - z'). \end{aligned} \quad (16)$$

Here $H(z - z')$ is the step-like Heaviside function. The accuracy of this approximation increases with the decreasing x and ζ .

We now substitute Eqs. (15) and (16) into Eq. (8), and combine the result with Eq. (4), to obtain the wave vectors defining the local peak position,

$$\begin{aligned} \tilde{q}_x(z) &= Q_x b_x \int_0^z dz' \rho(z'), \\ \tilde{q}_z(z) &= -\frac{2\nu}{1-\nu} Q_z b_x \int_0^z dz' \rho(z') - Q_z \frac{1+\nu}{1-\nu} \epsilon c(z). \end{aligned} \quad (17)$$

Finally, collecting the equations above, we can represent the x-ray scattering intensity as

$$\begin{aligned} I(q_x, q_z) &= \int_0^d dz \int_{-\infty}^{\infty} dx d\zeta e^{i\{[q_x - \tilde{q}_x(z)]x + [q_z - \tilde{q}_z(z)]\zeta\}} \\ &\times \exp \left[\int_0^d dz' \rho(z') \text{Re } \tau(x, z, \zeta, z') \right], \end{aligned} \quad (18)$$

where, in the approximation that we described above, $\text{Re } \tau = \text{Re}(\tau^{(1)} + \tau^{(2)})$, the two contributions are given by Eqs. (14) and (12), and we write their arguments as z and ζ instead of $z_1 = z$ and $z_2 = z + \zeta$.

The scans of constant q_x of the intensity distribution $I(q_x, q_z)$ on a RSM usually have well-defined maxima, we denote the positions of which as $q_{z \max}(q_x)$. Equations (17) approximately give, in the parametric form, the line $q_{z \max}(q_x)$. We simplify the fit of the experimental RSMs by defining this line on the experimental map and substituting corresponding values $q_{z \max}$ and $q_{x \max}$ instead of \tilde{q}_z and \tilde{q}_x into Eq. (17). Then, combining the two equations of Eq. (17), one can directly express $c(z)$ through $q_{z \max}$ and $q_{x \max}$. The value of z is obtained, in the current approximation for the dislocation density $\rho(z)$, by numerically solving the first equation of Eq. (17). We denote this value of z by z^* . That allows us to reduce the search from two unknown functions, $c(z)$ and $\rho(z)$, to the search of just one unknown function.

We can also make a rough estimate of the intensity $I(q_{z \max}, q_{x \max})$. Let us assume that the most essential contribution into diffraction intensity when integrating Eq. (18) over dz is given by a small vicinity of the point z^* . This assumption works better as the dislocation density increases and the integrand, as a function of z , becomes a sharp peaked function. Then, we can write

$$\begin{aligned} &\int_0^d dz e^{i\{[q_x - \tilde{q}_x(z)]x + [q_z - \tilde{q}_z(z)]\zeta\}} \\ &\approx \int_0^\infty dz \exp \left\{ i \left(\frac{d\tilde{q}_x(z)}{dz} x + \frac{d\tilde{q}_z(z)}{dz} \zeta \right) (z - z^*) \right\} \\ &\approx 2\pi \delta \left(\frac{d\tilde{q}_x(z)}{dz} x + \frac{d\tilde{q}_z(z)}{dz} \zeta \right). \end{aligned} \quad (19)$$

In this approximation, the integration over $dx d\zeta$ is reduced to the one-dimensional integration in the direction normal to the line $q_{x \max}(q_{z \max})$. If we make further severe approximation, assuming that w_{ij} and a_i are constants, we arrive at a notably simple relation

$$I(q_{x \max}, q_{z \max}) \propto 1 \left/ \frac{d\tilde{q}_z(z^*)}{dz} \right. \propto 1/\rho(z^*). \quad (20)$$

Qualitatively, Eq. (20) states that, the smaller is the dislocation density, the larger is the thickness of a sublayer contributing to diffraction intensity. However, Eq. (20) only qualitatively describes the experimental data. We used it to obtain the first approximation for further fit of the dislocation density profile.

III. X-RAY EVALUATION OF GRADIENT SEMICONDUCTOR STRUCTURES

Two samples, one with tensile and another with compression gradient layers have been grown using molecular

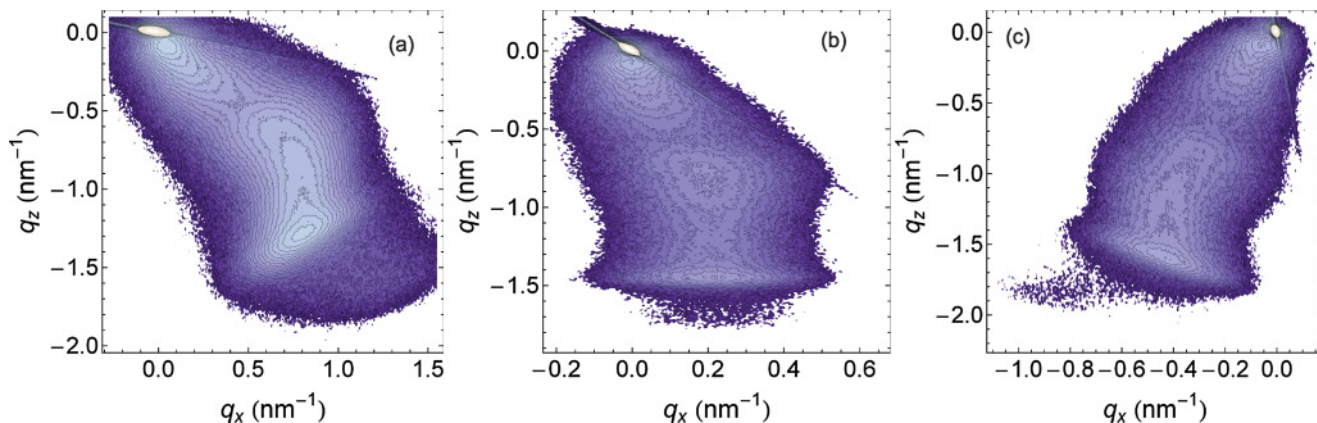


FIG. 1. (Color online) Experimental reciprocal space maps from sample 1 for 224^- (a), 004 (b), and 224^+ (c) Bragg reflections.

beam epitaxy (MBE). Sample 1 contains graded $\text{In}_x\text{Ga}_{1-x}\text{As}$ layer and sample 2 contains $\text{GaAs}_{1-x}\text{P}_x$ layer grown on 2 in. $\text{GaAs}(001)$ substrates. The growth was performed in a Riber 32 MBE system, which employed solid source effusion cells for gallium, indium, and dimeric arsenic. The substrate temperature was 510°C and the growth rate was ~ 500 nm/h. Both structures were grown with the concentration varying from zero at the bottom interface and increasing to $\sim 40\%$ at the top surface of the layer for sample 1 and $\sim 30\%$ for sample 2. The high-resolution x-ray diffraction RSMs were measured around 224^+ (the angle between the incident x-ray beam and the surface is larger than the angle between the exit beam and the surface), 224^- (the angle between the incident x-ray beam and the surface is smaller than the angle between the exit beam and the surface), and 004 Bragg reflections (see Figs. 1 and 2).

Before performing reconstruction of the concentration and relaxation profiles, the data was corrected for the possible crystallographic lattice tilt, using symmetric 004 RSMs and procedure described in Refs. 2 and 3 (see Fig. 3). For the sample 1, the tilt angles reached the value of 10° , and after correction, the lines $q_{x\text{max}}(q_{z\text{max}})$ for + and - geometries were aligned. For the sample 2, the tilt values are comparable with the angle uncertainty of the diffractometer.

Another factor to be taken into account in the calculation of diffracted intensity is a correction for peak broadening due

to instrumental effects. The resolution function $A(q_x, q_z)$ gives rise to a convolution integral

$$I_{\text{exp}}(q_x, q_z) = \iint dq'_x dq'_z A(q'_x - q_x, q'_z - q_z) I(q'_x, q'_z), \quad (21)$$

where $I(q'_x, q'_z)$ is the intensity distribution (18) that we have described above, and $I_{\text{exp}}(q_x, q_z)$ is the intensity measured in the experiment. We can proceed from the convolution to the product of Fourier transforms,

$$I_{\text{exp}}(q_x, q_z) = \iint dx dz e^{iq_x x + iq_z z} A_F(x, z) I_F(x, z). \quad (22)$$

The comparison of this expression with Eq. (18) shows that the effect of instrumental function can be taken into account without extra calculational efforts, just by multiplication of the correlation function by $A_F(x, z)$ in the right part of Eq. (18).⁶ We have determined the correlation function $A(q_x, q_z)$ by measuring the substrate reflection.

In order to extract composition and relaxation depth profiles, a fit of the experimental data to the calculation by Eqs. (17), (18), and (21) was performed. According to the discussion after Eq. (18), the dislocation density distribution $\rho(z)$ was fitted. The function $\rho(z)$ was specified by the values $\rho(z_i)$ at equally spaced points z_i . About ten points were taken first and a rough approximation for the profile $\rho(z)$ was found, providing a qualitative agreement between

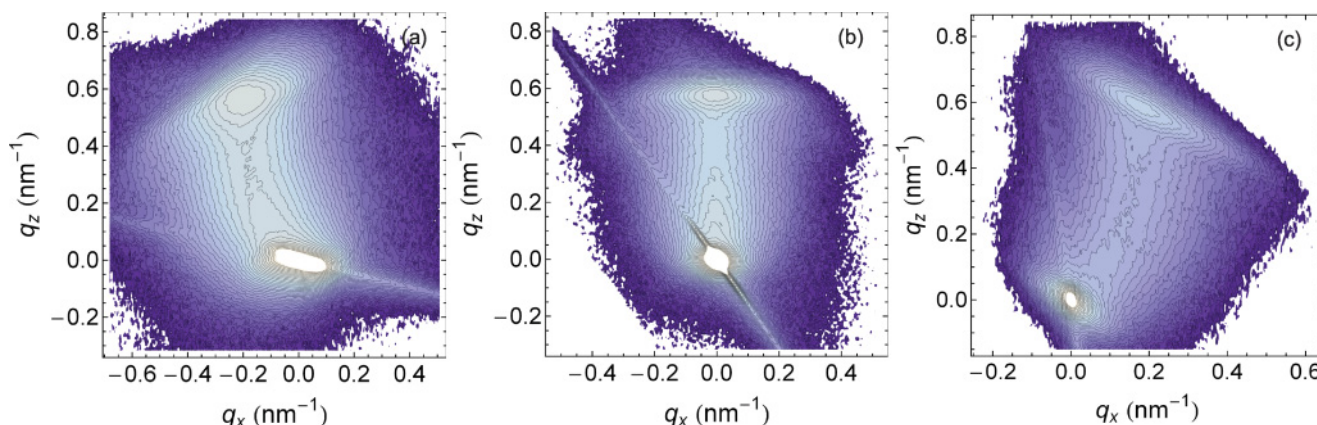


FIG. 2. (Color online) Experimental reciprocal space maps from sample 2 for 224^- (a), 004 (b), and 224^+ (c) Bragg reflections.

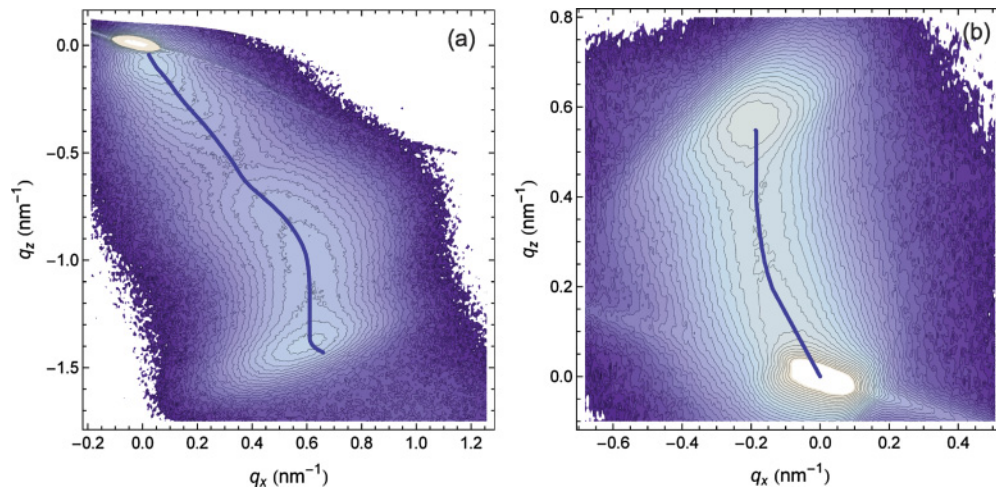


FIG. 3. (Color online) Measured 224⁻ RSMs from samples 1 (a) and 2 (b) after tilt correction. The blue line shows the positions of local maxima $q_{x \max}(q_{z \max})$ used for linking profiles $c(z)$ and $\rho(z)$ during data fitting procedure [see Eq. (17) and subsequent discussion].

calculated and experimental RSMs. The profiles following from approximations (19) and (20) were used as an initial guess. Then, the intermediate points z_i were introduced. For each point, one after one, the values $\rho(z_i)$ were chosen for best agreement between experimental and calculated RSMs. This sequential point-by-point fitting was performed several times until the fitted profile $\rho(z)$ remained almost unchanged after a single point-by-point fitting run.

Figure 4 shows the fit results for the Bragg reflection 224⁻ from samples 1 and 2. The calculations were performed for the 60° dislocations with the dislocation line directions [110] and $[\bar{1}10]$.

For sample 1, we expected from the nominal growth parameters the linear dependence of the concentration on thickness, with possible deviations from linear behavior at the lower interface of the layer. The results presented in Fig. 4(b) support this dependence. For some values of q_z , the calculated profiles are narrower than the experimental ones, even after convolution with the instrumental function. A possible reason for additional broadening of the experimental curves is a fluctuation of densities of dislocations with opposite sign of the tilt-related Burgers vector components.⁶ A similar broadening was also observed by Danis *et al.*⁵ The calculated intensity also deviates from the measured one at the origin, which is explained by essential contribution of the substrate peak broadened by the instrumental function.

From the growth parameters for sample 2, the linear dependence of the concentration on thickness is expected until the thickness of 1.8 μm , after which the concentration was kept approximately constant. Our calculation, see Fig. 4(b), confirms such concentration profile. There are obvious deviations in the region of small concentrations, where the contribution of the substrate peak is essential. The fitted profiles are slightly broader than the experimental ones. A possible reason may be a partial correlation of the dislocation positions.⁶

The proposed method provides the depth profiles $c(z)$ and $\rho(z)$ independently. There are several models describing the connection between these profiles.^{9,10,12,13} The minimization of elastic energy due to lattice mismatch and misfit dislocations

gives rise to^{9,10}

$$\rho(z) = \begin{cases} (\epsilon/b_x)dc(z)/dz, & 0 < z < z_c, \\ 0, & z > z_c. \end{cases} \quad (23)$$

In this approximation, the misfit strain is completely compensated up to critical thickness z_c , and there are no dislocations above z_c . The critical thickness z_c is given by the condition $\int_{z_c}^d \epsilon [c(z) - c(z_c)] dz = \lambda / (b_x \mu)$, where λ is the energy per unit length of dislocation, and μ is the appropriate elastic constant for biaxial strain. In the expressions above, Vegard's law is implied. The dislocation density of the form Eq. (23) was derived under assumption of complete thermodynamic equilibrium. However, it is commonly observed that the actual dislocation distribution deviates from it.³ In Fig. 4(c), the profiles $\rho(z)$ calculated from obtained concentration profile $c(z)$ according to Eq. (23) are shown by dashed lines. Corresponding dislocation densities obtained from RSMs are smaller in the region $z < z_c$. Also, the jump at $z = z_c$ is smeared out. Such deviations are expected since the evolution of dislocation distribution to equilibrium is not instant but takes place via plastic flow which is thermally activated kinetic process.^{12,13}

We note that the effect of dislocation correlations in the graded layers under investigation is minor. The experimental RSMs are quite well described under the assumption of uncorrelated dislocations. The same assumption was used in the previous studies of relaxed graded layers²⁻⁵ and also occurred accurate enough. This result contrasts with the case of uniform layers, where the misfit dislocations at the interface are highly correlated.⁶ These correlations give rise to the observed peaks notably (e.g., by a factor of 5) narrower than the ones calculated under assumption of uncorrelated dislocations. We conclude that in graded layers, where the misfit dislocations are distributed in the bulk of the film, the positional correlations between dislocations are much smaller than in uniform layers with dislocations at the interface.

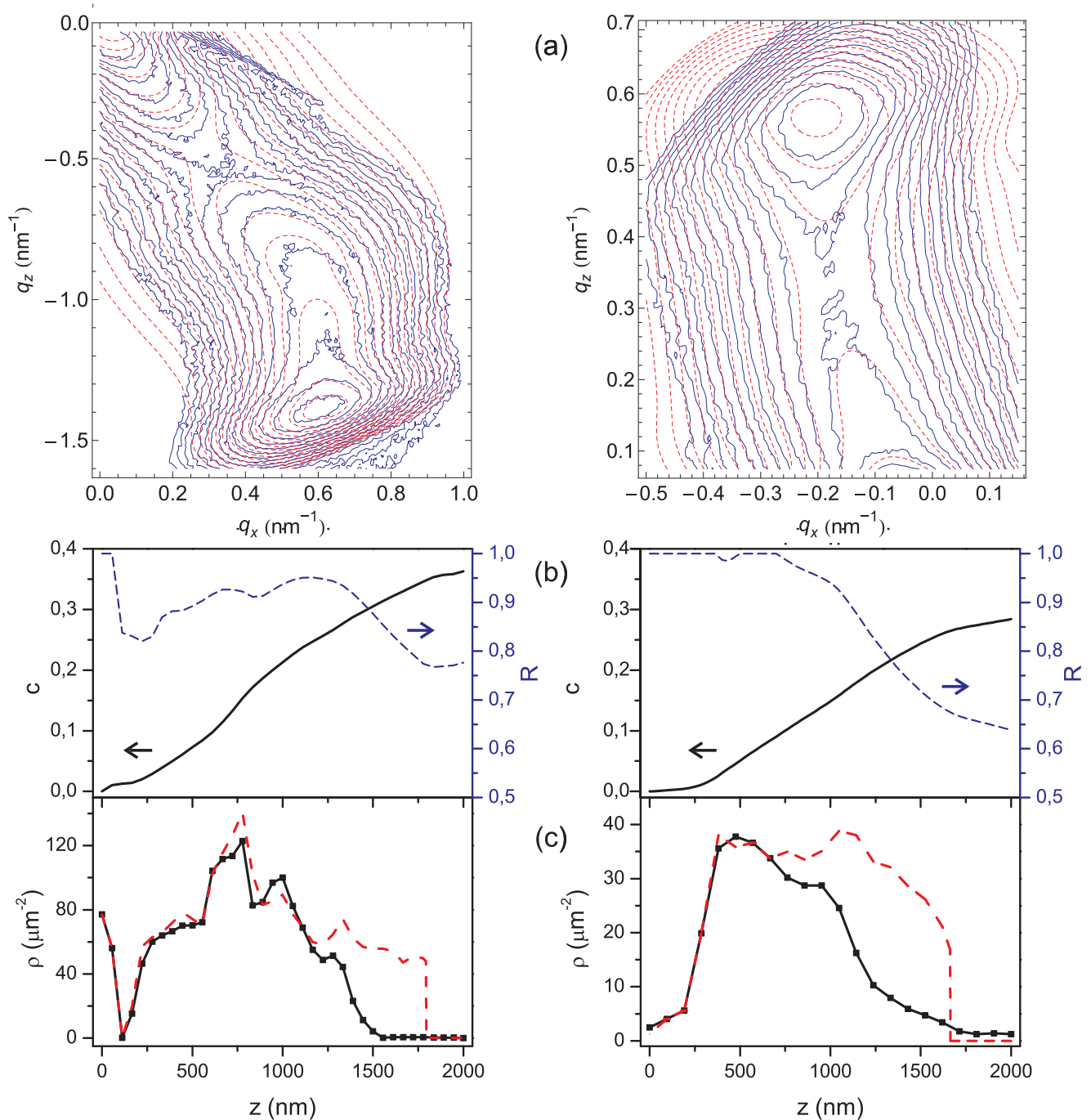


FIG. 4. (Color online) Results of RSM fitting for sample 1 (left) and sample 2 (right). (a) Contour plots of experimentally recorded (blue solid lines) and fitted (red dashed lines) intensity distribution from reflection 224⁻. The step of isointensity contours is 10^{0.1}. (b) Concentration and relaxation depth profiles. (c) The fitted misfit dislocation density (full line), black squares denote points $\rho(z_i)$ which were used for fitting. The dashed line corresponds to dislocation distribution according to model (Refs. 9 and 10).

IV. CONCLUSIONS

We show that the reciprocal space maps from graded epitaxial film contain enough information to obtain the concentration and relaxation depth profiles without any additional information. In the absence of a crystal lattice tilt, just single reciprocal space map in an asymmetric reflection is enough for such analysis. In the presence of crystal lattice tilt, the tilt corrections need to be done, which requires an additional

symmetric or an asymmetric RSM. Our RSM calculations are based on the kinematical x-ray diffraction theory from crystalline films with the misfit dislocation density depth profile. The theory is extended with respect to the case of the misfit dislocations located at interface. The concentration and relaxation depth profiles of $\text{In}_x\text{Ga}_{1-x}\text{As}/\text{GaAs}$ and $\text{GaAs}_{1-x}\text{P}_x/\text{GaAs}$ epitaxial graded films are determined by fitting of the experimental RSMs to the theoretically calculated ones. An accounting for the instrumental resolution function

is necessary for the correct data treatment. The obtained concentration profiles are found to be in a good agreement with the nominal profiles expected from the film growth conditions.

ACKNOWLEDGMENTS

We acknowledge I. D. Feranchuk (Belarusian State University, Minsk, Belarus) for helpful discussions.

-
- ¹U. Pietsch, V. Holy, and T. Baumbach, *High-Resolution X-Ray Scattering: From Thin Films to Lateral Nanostructures*, Advanced Texts in Physics, 2nd ed. (Springer-Verlag, New York, USA, 2004).
- ²V. Holy, J. H. Li, G. Bauer, F. Schaffler, and H.-J. Herzog, *J. Appl. Phys.* **78**, 5013 (1995).
- ³J. H. Li, V. Holy, G. Bauer, and F. Schaffler, *J. Appl. Phys.* **82**, 2881 (1997).
- ⁴K. D. Chtcherbatchev, A. D. Sequeira, N. Franco, N. P. Barradas, M. Myronov, O. A. Mironov, and E. H. C. Parker, *Mater. Sci. Eng. B* **91-92**, 453 (2002).
- ⁵S. Danis, V. Holy, J. Stangl, and G. Bauer, *Europhys. Lett.* **82**, 66004 (2008).
- ⁶V. M. Kaganer, R. Köhler, M. Schmidbauer, R. Opitz, and B. Jenichen, *Phys. Rev. B* **55**, 1793 (1997).
- ⁷M. A. Krivoglaz, *X-Ray and Neutron Diffraction in Nonideal Crystals* (Springer, Berlin, 1996).
- ⁸V. M. Kaganer and K. K. Sabelfeld, *Phys. Rev. B* **80**, 184105 (2009).
- ⁹J. Tersoff, *Appl. Phys. Lett.* **62**, 693 (1993).
- ¹⁰J. Tersoff, *Appl. Phys. Lett.* **64**, 2748 (1994).
- ¹¹V. M. Kaganer and K. K. Sabelfeld, *Acta Crystallogr. Sect. A* **66**, 703 (2010).
- ¹²B. W. Dodson and J. Y. Tsao, *Appl. Phys. Lett.* **53**, 2498 (1988).
- ¹³L. B. Freund and S. Suresh, *Thin Film Materials: Stress, Defect Formation and Surface Evolution* (Cambridge University Press, Cambridge, England, 2003).